Developing an Imaging System to Monitor Atom Traps for Neutral Atom Quantum Computing

A Senior Project

presented to

the Faculty of the Physics Department

California Polytechnic State University, San Luis Obispo

In Partial Fulfillment

of the Requirements for the Degree

Bachelor of Arts

by

Jenna Valdez

March, 2017

ABSTRACT

Quantum computing exploits the laws of quantum mechanics to exponentially increase computing rate for certain processes. A realized quantum computer could break encryptions and simulate large quantum systems previously unbreakable and unattainable with classical computers. Neutral atom quantum computing is a viable candidate for building these devices that satisfies four of the five criteria for a successful quantum computer. We are exploring a novel method in creating neutral atom qubits that involves a magneto-optical trap and a dipole trap created in the diffraction pattern behind an array of pinholes. The magneto-optical trap works to cool the atoms and centralize them into a cold-atom cloud in an ultra-high vacuum chamber. Laser light is then projected into the chamber through the array of pinholes, trapping the cooled atoms in light traps. In order to test the efficiency of our trapping method, I have developed an imaging system that monitors the atoms. The system is comprised of a high-speed camera that takes images of the trap while a photodiode measures the fluorescence signal from the cold-atom cloud. These measurements are used to determine the number of atoms successfully trapped, how long they remain trapped, and the trap frequency. This paper presents the details and process of developing the complete imaging system.

Table of Contents

List of Figures

1. Introduction

The field of quantum computation implements the principles of quantum mechanics into the world of computer science. The roots of its development date to the 1970s when researchers began attempts to control single quantum systems [1]. Specifically, researchers developed methods to "trap" single atoms in the interest of precisely determining an atom's behavior. In doing so, we are able to gain complete control over the system. Moving forward, we begin to expand these trapping methods into more complex systems.

Classical computers are constructed around the concept of a *bit*. These bits are units of information and in the computing field can have a state represented as either 0 or 1. Quantum computation is built around the concept of a quantum bit- or *qubit*. These qubits can have two states denoted as $|0\rangle$ and $|1\rangle$. The key difference between quantum and classical computing is that these qubits can also form any linear combination of states. The superposition of the qubit's basis states is written as:

$$|\psi\rangle_{1\text{-}qubit} = a|0\rangle + b|1\rangle$$

where a and b are complex numbers that satisfy

$$|a|^2 + |b|^2 = 1$$

This allows for an extreme increase in the number of inputs into the quantum computer.

In addition, two quibits can be entangled with each other. Entangled states cannot decompose into the product of single-qubit states, and any action performed on one qubit will affect the other. Entanglement allows to create two-quibit gates, making it essential in the operation of a quantum computer.

A successful quantum computer would implement a large amount of qubits (about 10^6) to create a system with certain capabilities far surpassing modern classical computational devices. Such advantages of a successful quantum computer include acquiring the ability to decrypt previously unbreakable cryptographic systems, building quantum simulations, and according to professor of mechanical engineering and physics at the Massachusetts Institute of Technology, Seth Lloyd, "understanding the fundamentally digital nature of the universe." [2]

Theoretical physicist David DiVincenzo identified the five criteria for the successful implementation of quantum computation [3]. The five criteria require that the system is scalable, readable, attains a long decoherence time, is able to initialize qubits into an initial state, and able to perform a universal set of quantum gates. In order to satisfy these requirements, we must create a system in which two qubits are able to strongly interact with each other while suppressing any interaction with their environment that leads to decoherence. One strategy in the attempts to create a quantum computer is neutral atom quantum computing. Neutral atoms are an ideal candidate for these quantum systems because they have little interaction with their surroundings, leading to long decoherence times[4]. Neutral atoms also have well characterized hyperfine states, so the quantum state is easily readable.

Creating these qubits from neutral atoms requires two methods of trapping: the Magneto-Optical Trap (MOT) followed by a light trap. MOT systems utilize laser cooling with strong magnetic field gradients to cool the atoms and bring them to a centralized location. Following the creation of this cold atom "cloud," a light pattern is projected into the vacuum chamber to trap the atoms so they are ready for quantum gate operations. After successful trapping, we

monitor the atoms using an imaging system that is able to determine how many atoms are trapped and for how long they remain trapped. The imaging system is the focus of my project.

This paper describes the development and implementation of an imaging system for the purposes of neutral atom quantum computing. In section 2, we will review the theoretical background of the MOT and light trap. Section 3 consists of the background to determine the number of trapped atoms, the details of the final optical setup of the imaging system, and the LabVIEW program that collects our data. Finally, section 4 contains a summary of the process of this project and my findings.

2. Theoretical Background for Cooling and Trapping Atoms

2.1 Magneto-Optical Trap

The magneto-optical trap works to cool our atoms to significantly decrease their speed and gather them into the center of an ultra-high vacuum chamber. Our MOT consists of the chamber, two lasers with wavelength of 780nm, and two opposing magnetic coils. This trap utilizes Doppler cooling to significantly slow the atoms and the Zeeman Effect to centralize them.

2.1.1 Doppler Cooling

In order to trap our atoms, we must first cool them so that they move at significantly slower speeds. Our experiment places Rubidium-87 atoms in an ultra-high vacuum chamber between the MOT coils where they are cooled to ~100μK. The atoms are cooled through the process of Doppler cooling. The Rubidium atoms are first hit with the laser light, causing them to absorb photons. The atom will then have a change of momentum of equal magnitude and in the same direction as the path of the photon. The atom spontaneously emits a photon in a

random direction, and because the atom continues to emit in all directions the momentum change caused by the emissions will cancel out. Therefore, the atom's net momentum shift is in the direction of the input of photons.

To better understand the Doppler cooling process, we further examine the absorption and emission cycles occurring in the atoms. Our trap involves two lasers: the trap laser and the pump laser. The trap laser works to excite the atoms and photons will spontaneously emit a short while later. An atom moving toward a laser will perceive higher frequency photons due to the Doppler Effect. To exploit this, we shift the frequency of the laser to below resonance frequency of the atom's electronic transition. The atoms moving toward this red detuned light are more likely to absorb photons because the Doppler Effect (illustrated in Figure 1) indicates that the photons and atoms will now have similar resonance frequencies.

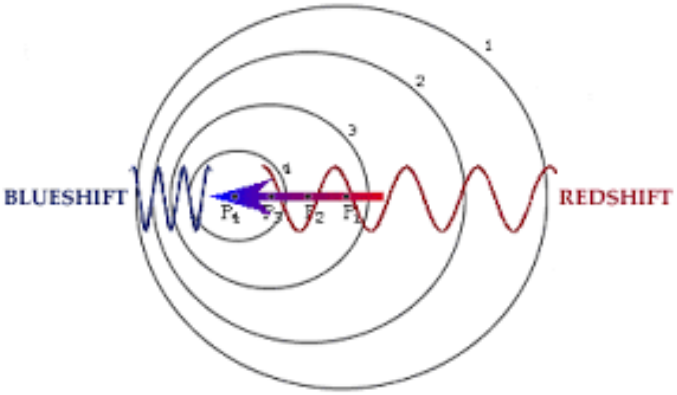

Figure 1: The Doppler Effect shifts frequency[5]

Each time the atom absorbs a photon, it will lose momentum equal to the momentum of the photon. This loss of momentum results in a decrease of kinetic energy, thus successfully slowing and therefore cooling the atoms. We send our lasers into the chamber along all three dimensions so that the atoms go through this process of laser cooling from all directions and are

adequately cooled regardless of their direction of travel. The atoms will therefore slow down but never speed up.

Figure 2 shows the electronic transition for our Rubidium-87 atoms associated with laser cooling advances from the F=2 of $5^2S_{1/2}$ hyperfine state to F=3 of $5^2P_{3/2}$. The electron will then decay back down to its initial state. This occurs for each absorption and continues to create decreases in momentum as the atom slows down. However, the atoms have some probability of going to the F=2 excited state and can then decay down to the F=1 state of $5^2S_{1/2}$. Due to selection rules, the electrons in this state cannot be excited up to the required state for Doppler cooling to take effect. This undesired transition is shown in Figure 2. The pump laser is used to correct this transition. This laser is tuned with a frequency that will excite electrons in the F=1 of $5^2S_{1/2}$ up to the F=2 state of $5^2P_{3/2}$. From this state, the electron is able to decay to the F=2 or F=1 state of $5^2S_{1/2}$ and can then be excited by the trap laser to the correct state for cooling.

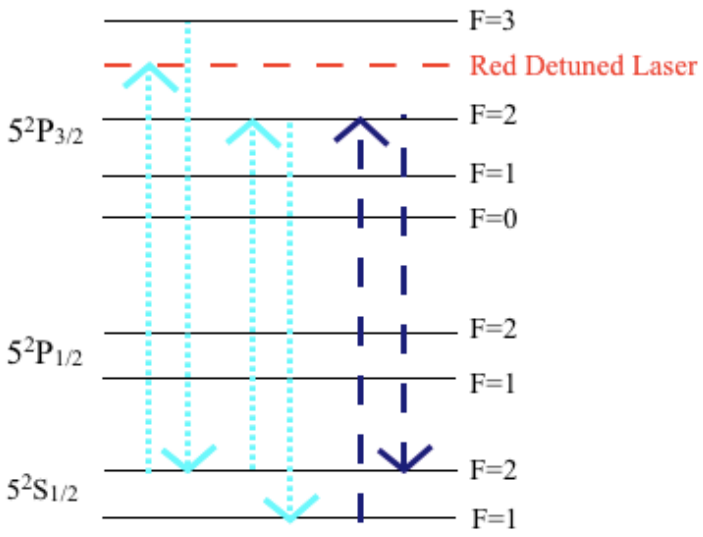

Figure 2: Hyperfine structure for Rubidium-87. The Doppler cooling process of our trap laser is represented in dotted turquoise. The second set of these lines is our undesired transition. The pump laser transition that corrects this is in dashed dark blue.

2.1.2 Zeeman Effect

The atoms are now sufficiently slowed, but must be centralized in the trap to create a cold atom cloud. We shift the atoms to the center by taking advantage of the Zeeman Effect- the splitting of energy levels that occurs in the presence of a magnetic field. The MOT setup includes two magnetic coils in a quadrupole configuration, a non-uniform magnetic field that is approximately zero in the center and strengthens linearly at further distances as shown in Figure 3.

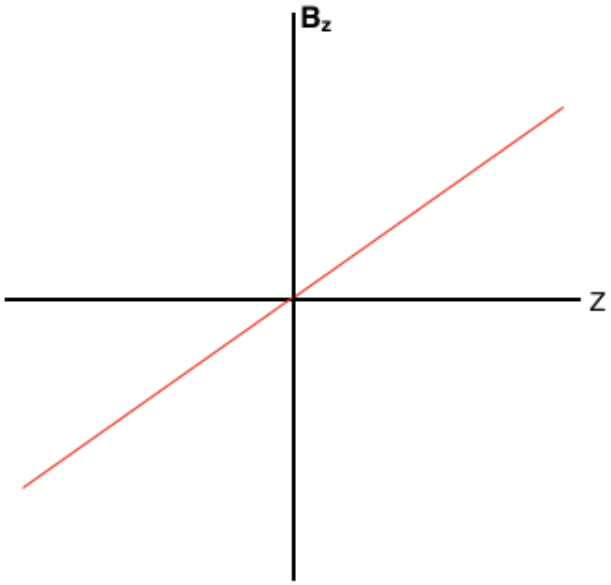

Figure 3: The trend in magnetic field strength moving further from the center Z_0

We set the magnetic coils with opposing directions of current parallel to each other. The magnetic field interacts with the magnetic dipole moment of the atoms. The interaction energy of the magnetic field with the magnetic dipole moment is given as:

$$\Delta E = \mu_B g m B_z \quad (1)$$

In equation 1, μ_B is the Bohr magneton, g is the Lande g-factor, m is the magnetic quantum number dependent on the z-component of the angular momentum of the atom, and B_z is the z-component of the magnetic field. We implement this concept into our trapping technique by shining two equally intense red-detuned laser beams into the trap along all three dimensions of space. We can further examine this process using the example of a simplified atom with total angular momentum J=1 and magnetic substates of m_j=-1,+1, and 0. Laser beams made of photons with a z-component of spin -1 can be expressed as σ- , and a beam with substate +1 is referred to as σ+. A beam with polarization σ- propagates along the positive z-direction; the σ+ beam propagates along the negative z direction. At a positive distance away from the center (z>0) , the frequency of the laser beams will be closer to resonance with the $m_j = -1$ than $m_j = 1$ state. The atoms at this positive z will thus be more likely to absorb a σ- photon and therefore receive a momentum kick from the σ- beam towards the center of the trap.

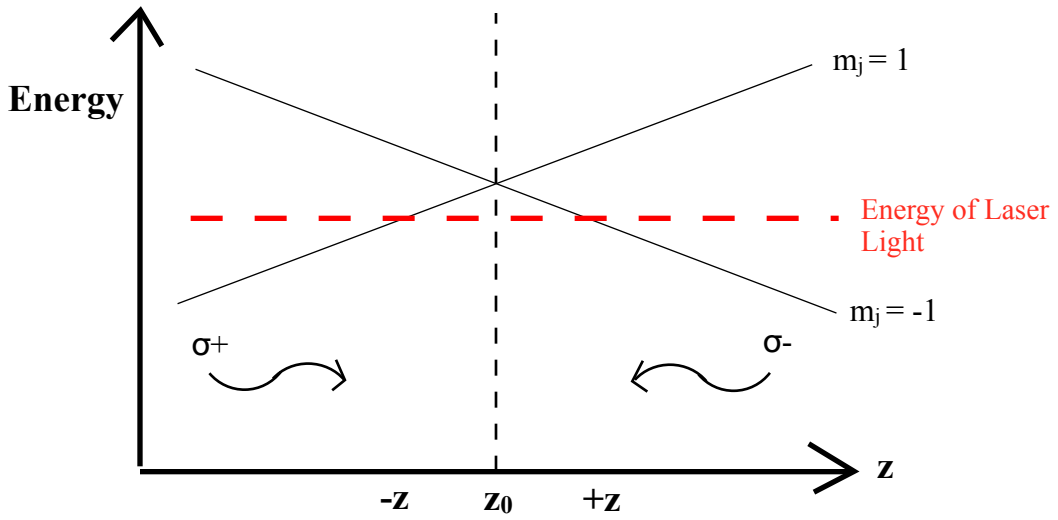

Figure 4: Zeeman split of the energy levels of the magnetic field present in the MOT with incoming polarized laser light

Conversely, at a point past the center of the trap ($z<0$), the photons are closer to resonance with the $m_j=1$ transition. They will therefore be more likely to scatter light from the $\sigma+$ beam, and receive a momentum kick in the opposing direction once again toward the center of the trap. The atoms are now cooled and centered in our MOT.

2.2 Light Traps

Once the cold atom cloud has been created, we are ready to transfer the atoms into the light traps. Within the cloud, atoms continue to absorb and emit photons. We turn off the magnetic field and MOT lasers and then project the light trap into the vacuum chamber. Gillen *et al.* propose a two-dimensional array of dipole traps so that the atoms can be individually addressed without disturbing the state of the surrounding atoms [6]. This method shines laser light through a pinhole, thus creating a diffraction pattern that contains local intensity maxima and minima [7]. These dark and bright spots correlate to potential energy wells into which the atoms become trapped. We can create a two-dimensional array by shining light through multiple pinholes and projecting it into our ultrahigh vacuum chamber [8]. The projected array of traps will allow manipulating individual atoms and perform operations We then use the imaging system to determine the number of atoms successfully trapped, and the lifetime and frequency of the trap.

3. Imaging System

3.1 Background for Monitoring Atoms in MOT

After our atoms have been trapped, we need an imaging system to monitor the success of their transition from the MOT to the dipole traps. The imaging system is able to determine how many atoms are successfully trapped and for how long they remain trapped by measuring the

fluorescence of the created cold atom cloud within the ultra-high vacuum chamber. While trapped in the MOT, the cooled atoms continue to absorb and spontaneously emit photons in all directions, resulting in the fluorescence of the cloud. After they have transitioned to the dipole traps, however, the atoms ideally do not fluoresce because the lasers used to trap them are detuned. Therefore, to monitor the location of the cloud we must make them fluoresce by shining a resonant MOT laser on to the atoms and then monitoring the fluorescence with two main components of the imaging system: a high-speed camera and a photodiode.

The fluorescence measured with our photodiode is proportional to the number of atoms in our trap. The voltage read by the photodiode is proportional to the rate at which the photons hit the active area of the photodiode. Our voltage reading therefore determines fluorescence, and can thereby be used to determine atom count. The rate of the photons hitting the photodiode can be determined by first establishing the number of photons emitted per atom per second- otherwise known as the scattering rate. The scattering rate is given by

$$\Gamma_{scat} = \frac{\left(\frac{I}{I_{sat}}\frac{\Gamma}{2}\right)}{1+\frac{I_0}{I_{sat}}+4\left(\frac{\Delta}{\Gamma}\right)^2} \qquad (2)$$

where I_o is the total intensity of the MOT laser beams and I_{sat} is the saturation intensity for Rubidium (1.64 mW/cm^2) [9]. Δ is the detuning and Γ is the natural line width of the $5^2S_{1/2}$ to $5^2P_{3/2}$ transition in Rubidium ($2\pi \times 6$MHz). Γ_{scat} will then produce the rate at which photons are spontaneously emitted over all angles. Using equation 2, the rate at which the photons hit the active area of the photodiode is reduced by the solid angle of the lens placed in front of the photodiode:

$$\Gamma_{det} = \frac{\pi r_{lens}^2}{4\pi l_{trap}^2} \Gamma_{scat} (.96)^2 \quad (3)$$

where r_{lens} is the radius of the lens (.5in), l_{trap} is the distance from the lens to the center of the MOT, and the factor $(.96)^2$ accounts for the reflectivity of the glass surfaces of the chamber that result in a 4% loss of photons at each interface. The reflectivity through the lens is negligible because the AR coating allows for transmission in excess of 99.5% [10]. The power incident on the photodetector due to all atoms in the MOT cloud is therefore:

$$P_{det} = hf\Gamma_{det} N \quad (4)$$

where hf is the energy per photon and N is the total number of atoms in the MOT. We can then solve for N in terms of the voltage reading from our photodiode (V_{det}), the photodiode's current per Watt of incident power (R_{det}), and the gain resistance of the photodiode that determines the output voltage (R_{gain}). The final expression for the number of atoms in the MOT is thus:

$$N = \frac{V_{det}}{hf\Gamma_{det} R_{det} R_{gain}} \quad (5)$$

where R_{det} is .57 Amps per Watt for our photodetector and R_{gain} is 10MΩ. The LabVIEW code that utilizes this formula is discussed in section 3.3.

3.2 Setup of Imaging System

3.2.1 Equipment Used in the Optical Setup

The imaging system uses a Basler piA640-210gm area scan high-speed camera and a photodiode built by former Cal Poly students [11]. The Basler camera takes 210 frames per

second and communicates with the computer via an Ethernet cable that is connected to a NI PCIe-8231 Gigabit Ethernet Interface Board. The photodiode (Photops UDT-555D) is connected to a National Instruments CB-68LP board read by the computer through a NI PCI-6014 data acquisition board to take in our voltage measurements.

3.2.2 Choosing Position of Photodiode and Camera

The first step in designing the experimental setup of the imaging system was to precisely determine the position at which the camera and photodiode should be mounted to minimize any reflected light from the lasers off of the glass of the vacuum chamber. The photodiode is placed above the camera as pictured below:

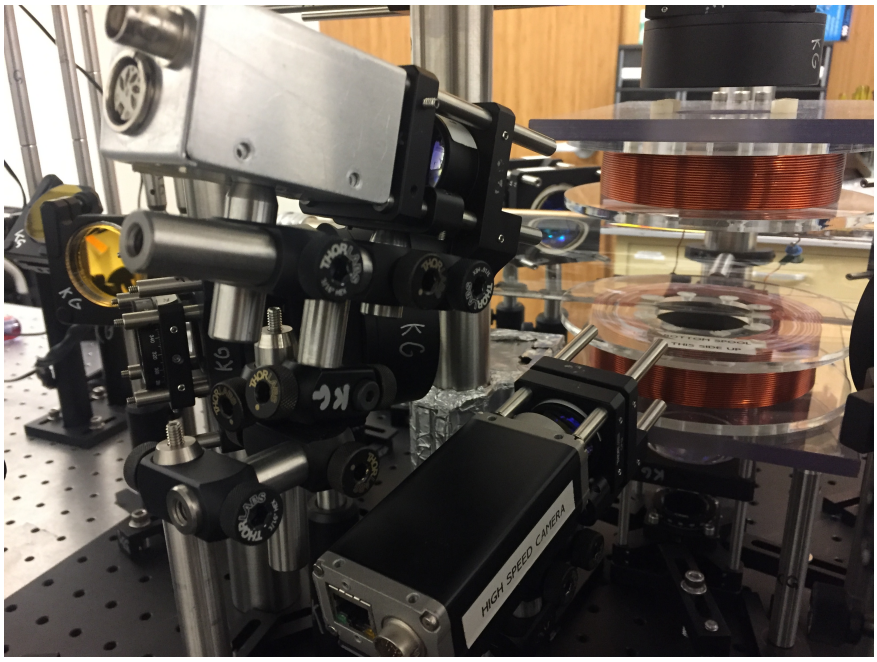

Figure 5: The photodiode and high-speed camera mounted in position, aimed at the center of our MOT

I first utilized geometrical optics to calculate the expected ideal distance between the lens and the face of both devices. This ideal image distance is calculated using the thin lens equation:

$$\frac{1}{f}=\frac{1}{s}+\frac{1}{s'} \tag{6}$$

Where *f* is the focal length of the lens, *s* is the distance between the center of the MOT and the lens, and *s'* is the distance between the lens and active area of each device. Figure 6 and 7 below illustrate the image and object distances for both the camera and photodiode setups.

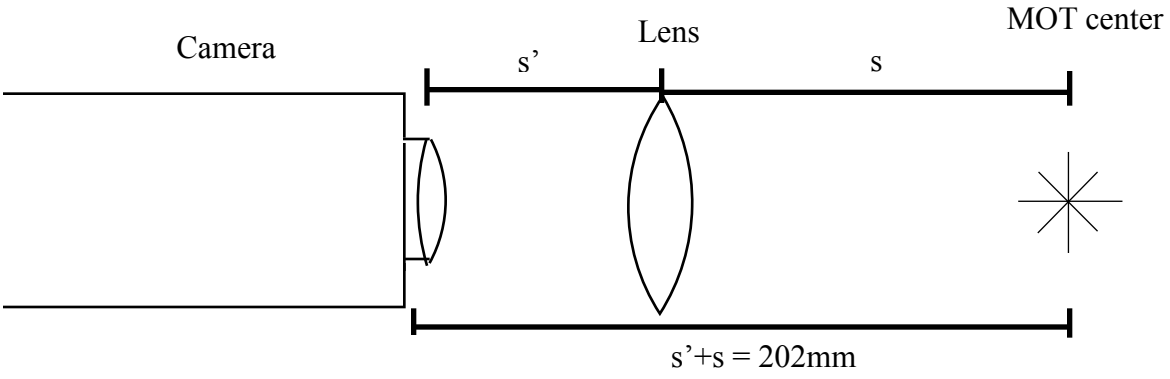

Figure 6: A schematic from camera to MOT center (figure not drawn to scale)

Using equation 6, we can solve for an optimal image *s'* for the camera

$$f(s')=\frac{(202mm\text{-}s')s'}{202mm} \tag{7}$$

Similarly, the setup and equation used to determine the ideal image distance is

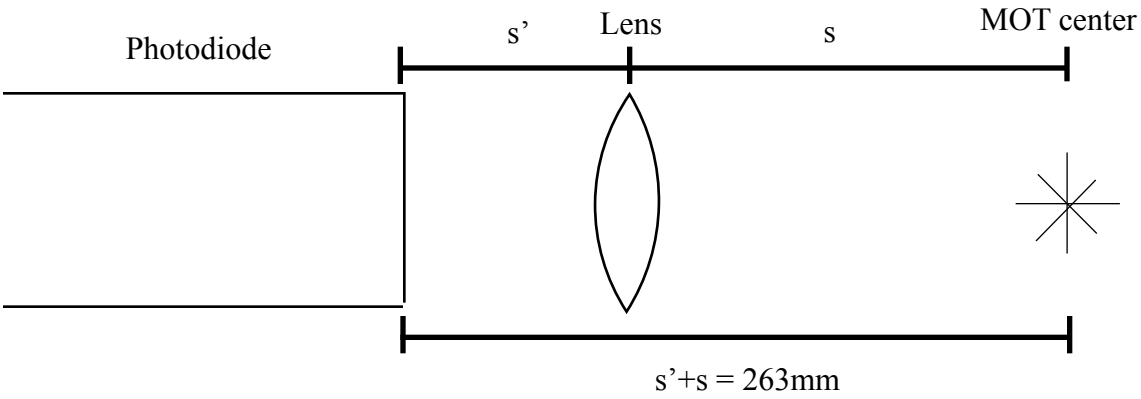

Figure 7: A schematic from photodiode to MOT center (figure not drawn to scale)

$$f(s') = \frac{(263mm - s')s'}{263mm} \tag{8}$$

The focal length for both setups is 25.4mm. Based on equation 7, the calculated image distance for the camera setup is then 30mm. Similarly, the image distance for the photodiode setup is calculated to be 28mm. I then conducted optical focusing tests based on these calculations. I watched the image on the computer while adjusting the lens position until it was perfectly focused. I verified that the lens should be placed 26 mm (±3mm) away from the camera. This discrepancy from the calculation is likely due to the thickness of the lens and human error in determining an optimally focused image. In order to determine the correct angle at which to aim the photodiode toward the center of the MOT, I switched out the photodiode with an alternate test camera and repeated the same test as with the Basler high-speed camera. I found the distance between lens and photodiode that would focus all light into the active area to be 25mm (±3mm).

I conducted a light test to ensure that my calculations and the camera test produced the correct distance between lens and photodiode. This test assures that all light that enters the lens also focuses on the active area of the photodiode, therefore confirming that the imaging system will produce an accurate atom count. In order to replicate the process, I placed a laser diode 238mm (the verified object distance) from the receiving lens on the photodiode cage system. This distance is the same as that which separates the photodiode and center of MOT during trapping, so the diode acts as a fluorescing atom cloud. Light from the cloud emits in all directions, so I conducted a visual test to ensure that in this mock test the light emitted by the

diode extended past the boundaries of the lens. A second visual test confirmed all light focused on to the photodiode's active area.

3.2.3 Developing Optimal Cage Systems for Photodiode and Camera

Both the camera and photodiode are placed in cage systems to create optical mounts that allow for horizontal adjustments between lens and device as well as height and angle adjustments. These systems are constructed around both the camera and photodiode so that one can easily aim the device toward the center of the MOT at the correct angle and move the lens the correct distance away while maintaining alignment from lens to active area. In the case of the photodiode, it was important to be able to switch out the photodiode with the alternate camera with ease when needed for testing. The face of the photodiode sits further back in the mount than the camera and also has a wider radius, so the cage system is constructed to allow for simple switching of photodiode and cage plate. Both systems are pictured below:

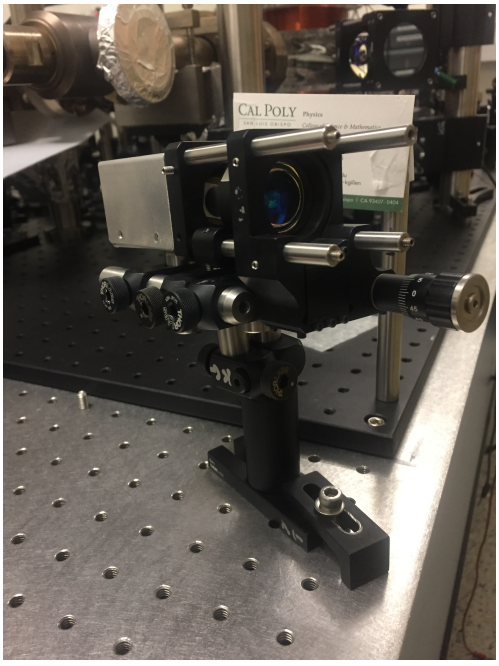

Figure 8: Final completed cage system for the photodiode

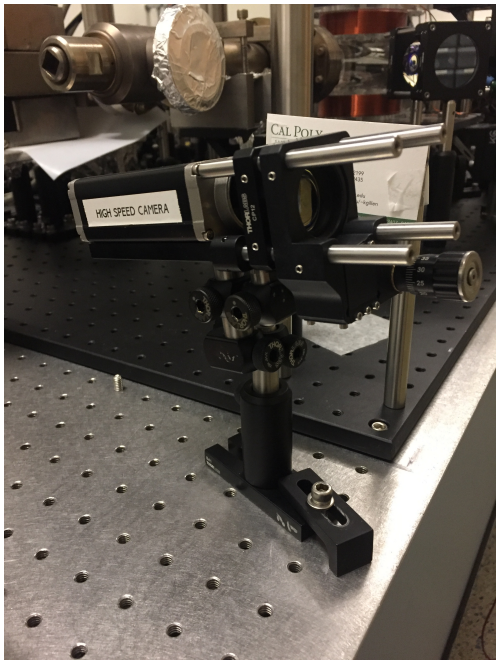

Figure 9: Final completed cage system for the high-speed camera

In our optical setup aimed at the MOT, the high-speed camera sits below the photodiode, aimed upward toward the center of the vacuum chamber. The cage setup includes the camera, a 25.4mm focal length plano-convex lens and CP12 lens mount to align the camera correctly so that it is aimed exactly through the center of the lens. The frame of the system is made up of mounting posts, fixed 90° clamp mounts, and a continuous 360° clamp mount to adjust the angle of the whole system. The lens is placed on a z-axis mount to precisely adjust the distance between lens and camera. The camera is attached to the base of the system directly by a mounting post. During the focusing tests for the camera, the z-axis mount was turned through its entire range and then meticulously adjusted until the image on the computer screen was in perfect focus. The optimal distance between the face of the camera and lens was determined to be 26mm. Images were recorded at each end of the z-axis range as well as mid-range to process and convert units of pixel across the image to distance measurements. This provides us with a conversion factor to determine the size of MOT cloud based on images taken with the camera. Thin rods are placed through a z-axis mount and an aligning lens mount to keep the system together.

Table 1: Equipment Used in High-Speed Camera Setup

Part Used	**THORLABS Part Number**
+25.4mm focal length lens	LA1951-B
Z-axis translation mount	SM1Z
Lens stabilizer	CP12
90° clamp mount (2)	RA90
360° clamp mount	SWC
Compact cage assembly rod, 3” (4)	SR3
Cage mounting bracket	CP02B

Optical post, 1”	TR1
Optical post, 2” (2)	TR2
Optical post, 3”	TR3

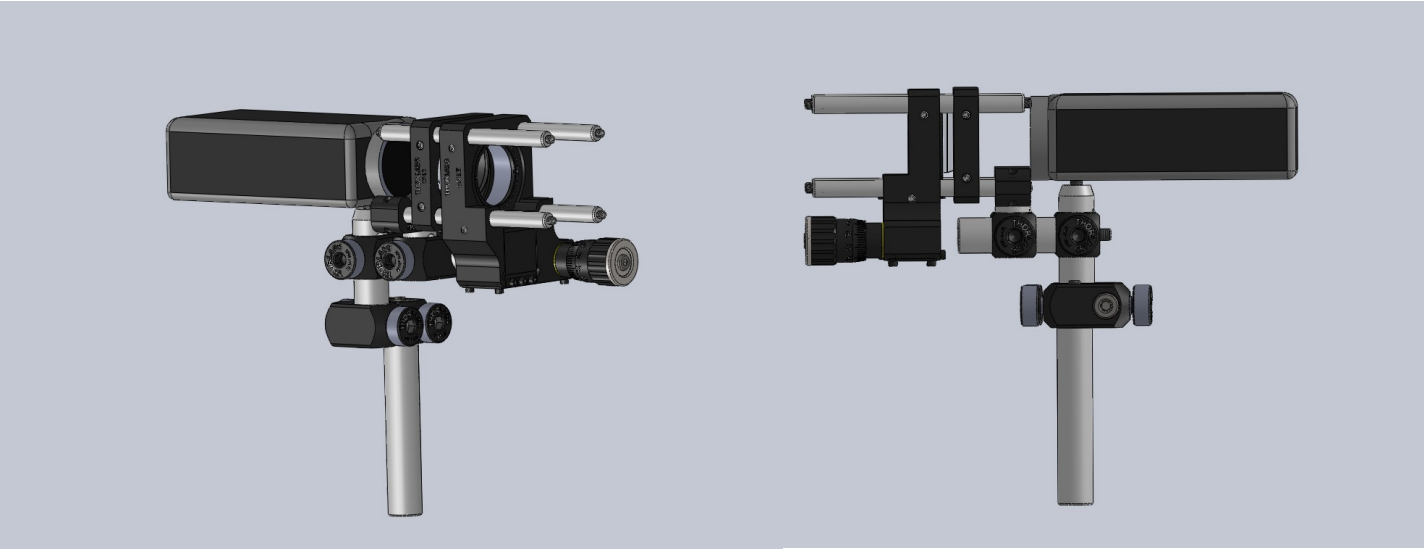

Figure 10: Assembly of the complete high-speed camera and cage system setup as created in SolidWorks

The photodiode has a more complex cage system because we must be able to easily switch out the photodiode for the camera designated for testing without disturbing the rest of the system. The frame is similar to that of the high-speed camera in that it is also constructed of mounting posts and adjustable clamp mounts, however the top portion of the cage system consisting of photodiode and lens is attached to the base of the system via the connective thin rods. This allows for easy transition from the photodiode to pop-in camera. When being used for trap measurements, the system includes the photodiode, a plano-convex lens with a focal length of 25.44mm, and Thorlabs CP06 aligning lens mount. The active area of the photodiode is surrounded by the opening of the aligning mount to align it with the center of the lens. The photodiode sits 25mm behind the lens. This distance was determined in a similar manner as the

high-speed camera. A pop-in camera was placed in the position of the photodiode and adjusted until the acquired image was precisely focused using the z-axis lens mount.

Table 2: Equipment Used in Photodiode Setup

Part Used	THORLABS Part Number
+25.4mm focal length lens	LA1951-B
Z-axis translation mount	SM1Z
Lens stabilizer	CP06
90° clamp mount (3)	RA90
360° clamp mount	SWC
Compact cage assembly rod, 3” (4)	SR3
Cage mounting bracket	CP02B
Optical post, 1”	TR1
Optical post, 2” (2)	TR2
Optical post, 3”	TR3
Optical post, 4”	TR4

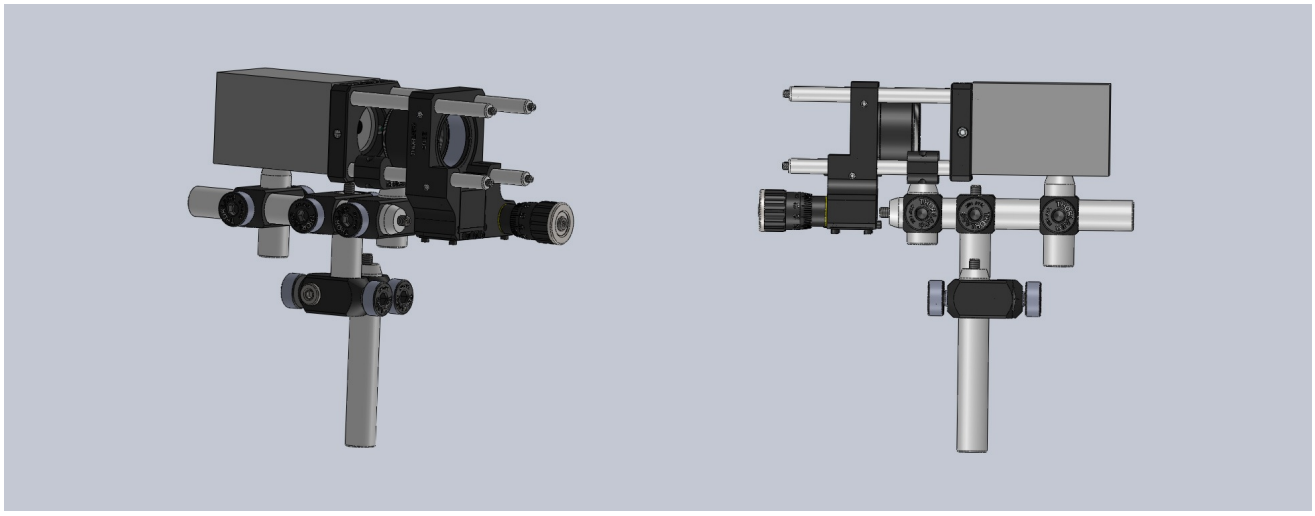

Figure 11: Assembly of the complete photodiode and cage system setup as created in SolidWorks

During tests, the photodiode is switched with the camera, and we must replace the aligning mount with one that has a larger diameter because the rim that surrounds the test camera's active area is wider than that of the photodiode. The final cage system setup utilizes only the thin rods running horizontal on the top portion of the system for the transition. To switch from photodiode to camera, we must first remove the device by sliding it off the rods in the opposite direction from the lens. We remove the CP06 aligning mount and then replace it with a CP12 mount in the same placement as the previous. Finally, we place the camera into the 90° mount clamp and adjust it forward so that its face is flat against the mount.

3.3 LabVIEW Program

As discussed in section 3.1, the number of atoms we successfully trap can be determined from the voltage reading of our photodiode. In order to read out our data, I expanded on a LabVIEW program written by Taylor Shannon that captures and saves camera frames and photodiode readings [11]. This original program stores a camera frame of 640x480 pixels every 4.7 milliseconds, and the photodiode voltage readings are read from the NI PCI-6014 data acquisition board and stored into an array. My addition to the program sends the photodiode reading and relevant variables through the series of equations 2, 3, and 5 to determine the number of atoms trapped and saves the output reading into the requested file path. The full block diagram is shown in Figure 12. In addition, the program is written so that future users can adjust any of the variables including radius of the lens in front of the photodiode, distance from lens to MOT, and the total laser intensity and detuning that is determined on the day of trapping.

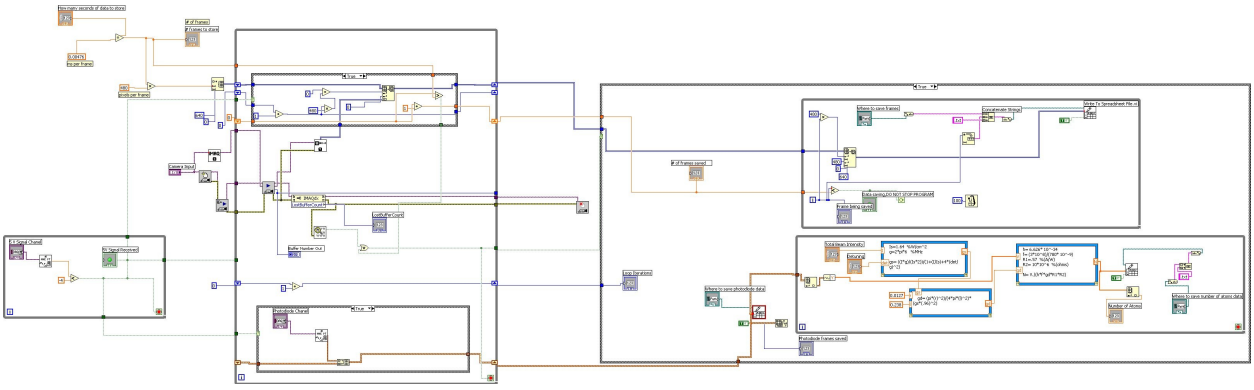

Figure 12: Complete block diagram that captures camera frames and photodiode voltages and calculates total number of atoms trapped

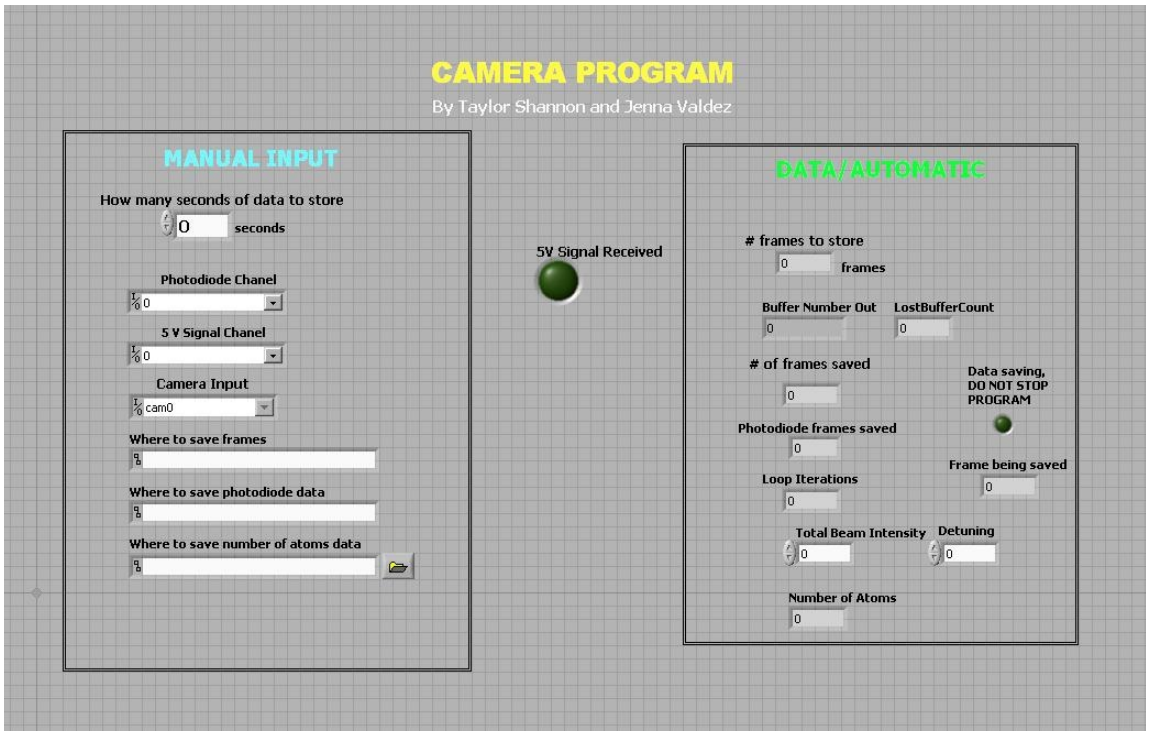

Figure 13: Front panel for LabVIEW program

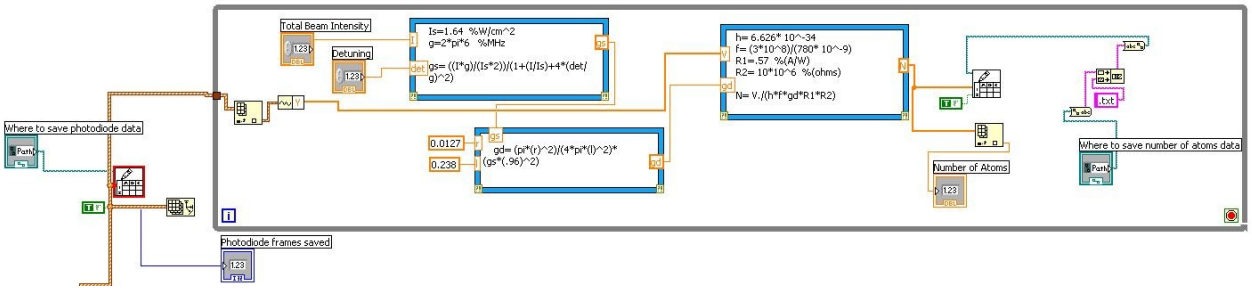

Figure 14: A close up of the addition to the LabVIEW program that sends the photodiode readings through a sequence of equations to output total number of atoms

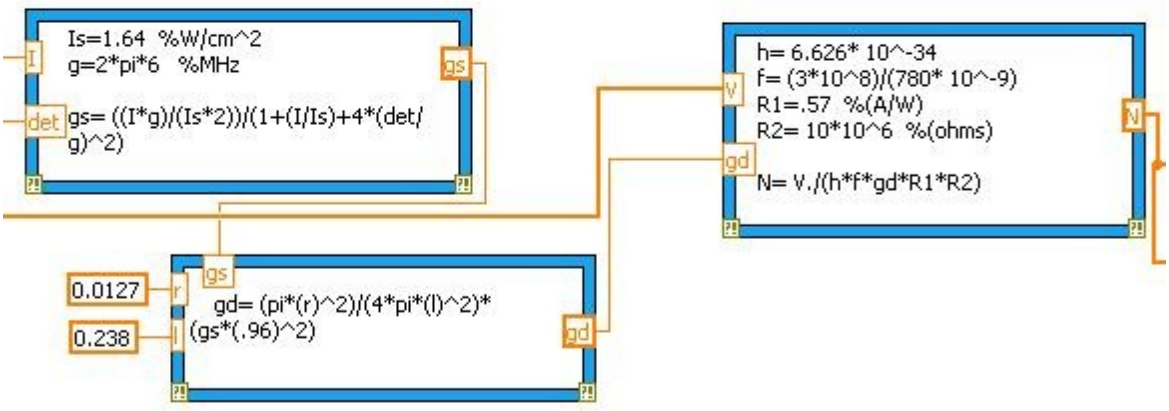

Figure 15: A close up of the Mathscript functions that use input variables to output final atom count (N)

4. Conclusion

The creation of a true quantum computer would mean transcending the limits of modern computing power. According to DiVincenzo's five criteria, neutral atom quantum computing is an ideal candidate for a successful quantum system. Our method utilizes neutral Rubidium atoms as qubits by first trapping the atoms in a cool and centralized cloud in the vacuum chamber of a magneto-optical trap. A light pattern will then be projected through an array of

pinholes and into the chamber to trap the cooled atoms in dipole traps. I have designed and implemented an imaging system that will be able to determine how many of the atoms are successfully trapped by the light, and for how long they remain trapped. The imaging system consists of a high-speed camera and a photodiode. I also designed and engineered cage systems for both devices to ensure alignment, simple lens adjustments, and the ability to precisely position the photodiode and camera aimed at the center of the MOT. The camera is used to determine the size of the created cold atom cloud, and the photodiode measures the voltage across the cloud and sends the data through a LabVIEW program that will output the atom count. Looking forward, the information acquired by the imaging system will determine the success of the trap. A successful trap will be a testament to the pinhole array method for neutral atom quantum computing and an advance toward the realization of quantum computers.

Work Cited

[1] Nielsen, Michael, and Isaac Chuang. Quantum Computation and Quantum Information. Cambridge: Cambridge UP, 2000.

[2] Palmer, Roxanne. "How Quantum Computing Could Change Everything." The Week. N.p., 28 Oct. 2014. Web. 24 Feb. 2017. <http://theweek.com/articles/443104/how-quantum-computing-could-change-everything>.

[3] DiVincenzo, David. “The Physical Implementation of Quantum Computation.” IBM T.J. Watson Research Center, (2008).

[4] Brennen, Gavin, Ivan Deutsch, and Poul Jessen. "Quantum Computing with Neutral Atoms in an Optical Lattice." Fortschr. Phys. 48, (2000).

[5] The Doppler Effect. Digital image. NCSA. University of Illinois, 1995. Web.

[6] Gillen-Christandl, Katharina, and Bert Copsey. “Polarization-dependent atomic dipole traps behind a circular aperture for neutral-atom quantum computing.” Physical Review A 83. 023408 (2011).

[7] Christandl, Katharina, Glen Gillen, and Shekhar Guha. "Optical dipole traps for cold atoms using diffracted laser light." Physical Review. A 74.013409 (2006).

[8] Gillen-Christandl, Katharina, and Glen D. Gillen. “Projection of diffraction patterns for use in cold neutral atom trapping.” Physical Review A 82, 063420 (2010).

[9] Metcalf, H.J. and P. van der Straten, Laser Cooling and Trapping. 1999, New York: Springer-Verlag. Table C

[10] “N-BK7 Plano-convex Lenses (650-1050nm) Features” https://www.thorlabs.us/newgroup-page9.cfm?objectgroup_id=3280&pn=LA1951-B

[11] Shannon, Taylor. Monitoring Atoms for Neutral Atom Quantum Computing. Cal Poly, Mar. 2014.